Sentinel-2 time series reveal species-specific responses in temperate conifer dieback

Hélène Carletti, Jean-Claude Gégout, Raphael Dutrieux, Jean-Baptiste Féret, Cédric Vega, Thierry Belouard, Anne Jolly, Juliette Cansell, Christian Piedallu

▶ **To cite this version:**

Hélène Carletti, Jean-Claude Gégout, Raphael Dutrieux, Jean-Baptiste Féret, Cédric Vega, et al.. Sentinel-2 time series reveal species-specific responses in temperate conifer dieback. European Journal of Remote Sensing, 2025, 58 (1), pp.2547386. ⟨10.1080/22797254.2025.2547386⟩. ⟨hal-05223935⟩

HAL Id: hal-05223935

https://hal.science/hal-05223935v1

Submitted on 26 Aug 2025

HAL is a multi-disciplinary open access archive for the deposit and dissemination of scientific research documents, whether they are published or not. The documents may come from teaching and research institutions in France or abroad, or from public or private research centers.

L'archive ouverte pluridisciplinaire **HAL**, est destinée au dépôt et à la diffusion de documents scientifiques de niveau recherche, publiés ou non, émanant des établissements d'enseignement et de recherche français ou étrangers, des laboratoires publics ou privés.

Distributed under a Creative Commons CC BY 4.0 - Attribution - International License

Sentinel-2 time series reveal species-specific responses in temperate conifer dieback

Hélène Carletti[1,2 *], Jean-Claude Gégout[1], Raphael Dutrieux[3], Jean-Baptiste Féret[3], Cédric Vega[4], Thierry Belouard[5], Anne Jolly[6], Juliette Cansell[7], Christian Piedallu[1]

1. Université de Lorraine, AgroParisTech, INRAE, UMR Silva, 54000 Nancy, France
2. Agence de l'environnement et de la Maîtrise de l'Energie 20, avenue du Grésillé- BP 90406 49004 Angers Cedex 01 France
3. TETIS, INRAE, AgroParisTech, CIRAD, CNRS, Université Montpellier, 34093 Montpellier, France
4. Université Gustave Eiffel, ENSG, IGN, Laboratoire d'Inventaire Forestier, 14 rue Girardet, F-54042, Nancy, France
5. Département de la santé des forêts, UMR Biodiversité Gènes et Communautés, INRAE, 33610 CESTAS, France
6. Office National des Forêts, département Recherche Développement Innovation, pôle de Nancy, 54000 Nancy, France
7. Centre National de la Propriété Forestière (CNPF) Grand Est, 54000 Nancy, France

*Corresponding author: Hélène Carletti, helene.carletti@agroparistech.fr

*email addresses:

Jean-Claude Gégout, jean-claude.gegout@agroparistech.fr

Raphael Dutrieux, raphael.dutrieux@gmail.com

Jean-Baptiste Féret, jean-baptiste.feret@teledetection.fr

Cédric Vega, cedric.vega@ign.fr

Thierry Belouard, thierry.belouard@inrae.fr

Anne Jolly, anne.jolly@onf.fr

Juliette Cansell, juliette.cansell@cnpf.fr

Christian Piedallu, christian.piedallu@agroparistech.fr

Highlights

- Anomalies on Times-series of Sentinel-2 data allow to characterise forest decline
- The performance of dieback detections depends on species and vegetation indices used
- Detection performed better in pure than in mixed stands, especially for Norway spruce
- Early warning dieback detection performs better for silver fir

Abstract

Silver fir (Abies alba Mill.), Norway spruce (Picea abies (L.) H. Karst) and Scots pine (Pinus sylvestris L.) are three major conifer species in Europe that are currently experiencing severe dieback. Developing effective monitoring of these species over large areas and at high temporal frequencies is essential to assess their mortality dynamics. Multispectral satellites have demonstrated their effectiveness in identifying mortality patterns for different functional types, but differences among species remain poorly addressed. Using Sentinel-2 time series and ground observations collected between 2018 and 2023 over the French mountains for 742 pure and 949 mixed stands, we investigated the interest of analysing dieback detection at the species

level. We used spectral time series analysis from seven raw bands and eight vegetation indices and integrated spectral anomalies for different periods prior to the ground survey. Results differed significantly among species: the best performance was obtained for silver fir with a fifteen-month period and Inverted Red-Edge Chlorophyll Index (IRECI), for Norway Spruce with a one-month period and Continuum removal of the shortwave-infrared spectrum (CRSWIR), and for Scots pine with a four–month period and red-edge (CRRE). In pure stands, the time series analysis detected Norway spruce dieback better (R^2 = 0.54, OA=77%) than it did Silver fir (R^2 = 0.34, OA=61%) or Scots pine (R^2 = 0.16, OA=64%). Dieback was difficult to detect in its early warning stages and in mixtures mainly for Norway spruce and Scots pine. This study highlights the importance of developing species-specific methods for large-area monitoring of dieback.

Keywords

Time series, Sentinel-2, dieback, Norway spruce, silver fir, Scots pine

Introduction

Forests provide multiple ecosystem services including wood production, hydrological regulation, carbon sequestration and recreational activities (Millennium Ecosystem Assessment, 2005) are being threatened by the recent increase in forest mortality observed in many parts of the world, including Europe (Senf et al., 2020). Dieback is a multifactor phenomenon linked to a general, progressive degradation of tree health, and result in higher than usual tree mortality (Allen, 2009). The factors involved include predisposition (e.g. tree age, soil compaction), external abiotic conditions (e.g. storms, drought, frost) and biotic events (e.g. fungi, insect outbreaks) (Manion, 1981). Climate change is also contributing to the recent

upward shift in mortality trends worldwide through increasingly intense and frequent extreme climatic events (Senf et al., 2020) and biotic threats (Seidl et al., 2017). Historically, the health of forests has been assessed using inventories that express the severity of dieback through various symptoms (Lausch et al., 2017; Taccoen et al., 2019). Among them, foliar loss leading to an increase in canopy transparency, and dead outer and upper branches are the most frequently observed. These can lead in extreme cases to the death of the tree (Pontius & Hallett, 2014). Most forest health inventories rely on a systematic sampling design. They may not always accurately reflect dieback patterns due to the localised nature of some mortality events and to the harvesting of dead trees prior to sampling. Because they are too sparse to map dieback at a fine scale, remote sensing may provide valuable complementary information essential to robust decision-making (Hartmann et al., 2018). Multispectral data are the most widely used for forest dieback assessment (Torres et al., 2021). Currently, operational multispectral missions provide global coverage with a short revisit period, and medium to high spatial resolution. Spectral information over multiple bands makes it possible to distinguish the specific characteristics of forest canopies. Photosynthetically active pigments influence reflectance in the visible domain (VIS, 400-700 nm), leaf structure and canopy structure influence reflectance in the near infrared domain (NIR, 700-1100 nm), and absorption features from plant water content act in the shortwave infrared domain (SWIR, 1100–2400 nm) (Carter & Knapp, 2001; Gitelson & Merzlyak, 1998; Kokaly et al., 2009). Spectral bands can be used alone or in combination with vegetation indices (VIs). The latter approach maximises sensitivity to specific vegetation properties, often associated with a specific part of the electromagnetic spectrum, and minimises sensitivity to other factors (e.g., atmospheric conditions, acquisition geometry) (Jackson & Huete, 1991). VIs have been widely used to assess forest dieback, and perform better than spectral bands (Bárta et al., 2021). Dense satellite-image time series (SITS) are now outperforming single-image-based approaches to forest

dieback monitoring (Torres et al., 2021). SITS are used to model the normal behaviour of spectral indices over time for a given site, then to compare this with current values to identify spectral anomalies. The greater the difference over a period of time, the more important the changes in stand fitness are likely to be. Detecting change with continuous SITS provides an unprecedented opportunity for real-time monitoring (Woodcock et al., 2020). Algorithms have been developed to monitor forest change from Landsat time series, such as LandTrendr, BFAST or CCDC-SMA (Kennedy et al., 2010; Verbesselt et al., 2010; Chen et al., 2021). Their performance depends in part on the availability of cloud-free data, which is necessary to properly characterise the seasonality of the signal. This is particularly important in cloudy humid regions such as mountainous areas (Lastovicka et al., 2020). Comparisons between time series from satellite missions have shown differences in their ability to predict conifer forest dieback. Sentinel-2, which has a high spatial resolution and revisit period, provides in general better results (König et al., 2023). Most existing studies distinguish only a few dieback classes, often only one degraded stage and a contrasting healthy stage (Abdullah et al., 2019a). Studying the shape of the transition between the normal health status and strong dieback symptoms (Trumbore et al., 2015) requires detailed gradients covering all the stages of dieback, especially when visible symptoms are moderate (crown defoliation, presence of dead branches, ...), i.e. the early warning stages, which are often omitted despite their importance for managers (Torres et al., 2021). Few studies have evaluated remote sensing approaches on a detailed dieback gradient with a description of tree dieback status based on ground survey observations (Hawryło et al., 2018). Most remote sensing studies on dieback have focused on one tree genus, such as Pinus or Quercus, or one functional type, as it is quite difficult to distinguish tree species over large areas (Gallardo-Salazar et al., 2023; Drechsel & Forkel, 2025). A few specific studies in contexts with enough pure stands have focused on a single species (Bárta et al., 2021; Marx & Kleinschmit, 2017); this simplifies detection since responses to stress differ among species. For

example, Radeloff et al. (1999) showed that the NIR reflectance of Pinus banksiana was greater than that of other conifer species and that it tended to increase with stress, whereas it decreased in other conifer species (Abdullah et al., 2019b). This suggests that detection performances should be improved by selecting the method and spectral index according to the target species (Ye et al., 2021). Selecting only pure stands is recommended to study single-species responses (Radeloff et al., 1999); however, 70% of the forests in Europe consist of multi-species stands (UNECE & FAO, 2011). Integrating species differences and mixture effects into satellite data analysis is quite challenging and is a limiting factor for current dieback detection algorithms (Bárta et al. 2021). We aimed to investigate how the responses of species belonging to the same functional group differ at different levels of mixture and dieback in time-series dieback monitoring. We focused on silver fir (Abies alba Mill.), Norway spruce (Picea abies (L.) H. Karst) and Scots pine (Pinus sylvestris L.), representative of the three most important conifer genera in Europe (Strona et al., 2016). We used an anomaly detection method and compared different spectral bands and vegetation indices over different time periods to evaluate their performance in predicting dieback gradients for pure stands of each species. The most efficient vegetation index for each species was retained, and its ability to predict dieback gradients was then evaluated for different levels of species mixture.

Materials and methods

Study area

We evaluated silver fir, Norway spruce and Scots pine dieback on plots located throughout the southwestern part of their geographical range, in five mountain ranges (the Vosges, the Jura, the Massif Central, the Alps and the Pyrenees), as well as the surrounding areas, which are all located in France. The elevations in the studied forests range from 80 to 2,100 meters, with an average of about 900 meters. Mean annual precipitation during the study period varied from 650 mm to 2,100 mm, with an average of 1,100 mm. Mean annual temperatures ranged from

2.5 degrees to 15.0 degrees with an average of 8.7 degrees (Piedallu et al., 2016). Four of the mountain ranges (Vosges, Massif Central, Alps and Pyrenees) are composed of crystalline and calcareous rocks, while the Jura is only calcareous. Forests cover approximately 40% of the study area (i.e. 10M ha), of which 26 % is coniferous, 58 % is deciduous, and the remaining 16% is mixed coniferous/deciduous forest (IGN, 2019). Approximately 57% of the forest area is composed of multiple species (Bontemps et al., 2019), and silver fir, Norway spruce and Scots pine make up 83% of the coniferous forest (IGN, 2019).

Data collection

Ground observations

We used a subset of 1,773 French National Forest Inventory (NFI) plots, surveyed from 2018 to 2023, containing at least one dominant or co-dominant tree of our target species (Vidal et al., 2005). They provide circumferences and species names for each tree with a diameter greater than 7.5 cm and ecological information on a circular plot of 15 metres with continuous tree cover (i.e. without discontinuities such as roads). The selected plots showed no signs of management intervention or decline due to extreme events (fire, windthrow…) in the five years prior to the survey. We focused on declining changes such as insect- or drought-induced dieback and therefore excluded plots affected by other extreme events (windthrow, fire, avalanche…) (Fig.1) (Ye et al., 2021). As dieback symptoms are rarely observed in systematic large-area monitoring, we added 191 plots across the area that were specifically surveyed for forest dieback, and provide information on tree species and circumferences (Fig.A.1) (Gilles et

al., 2024). The NFI plots have a surface area of 700 m² and the additional plots ranged from 300 m² to 6300 m² (average 1000 m²).

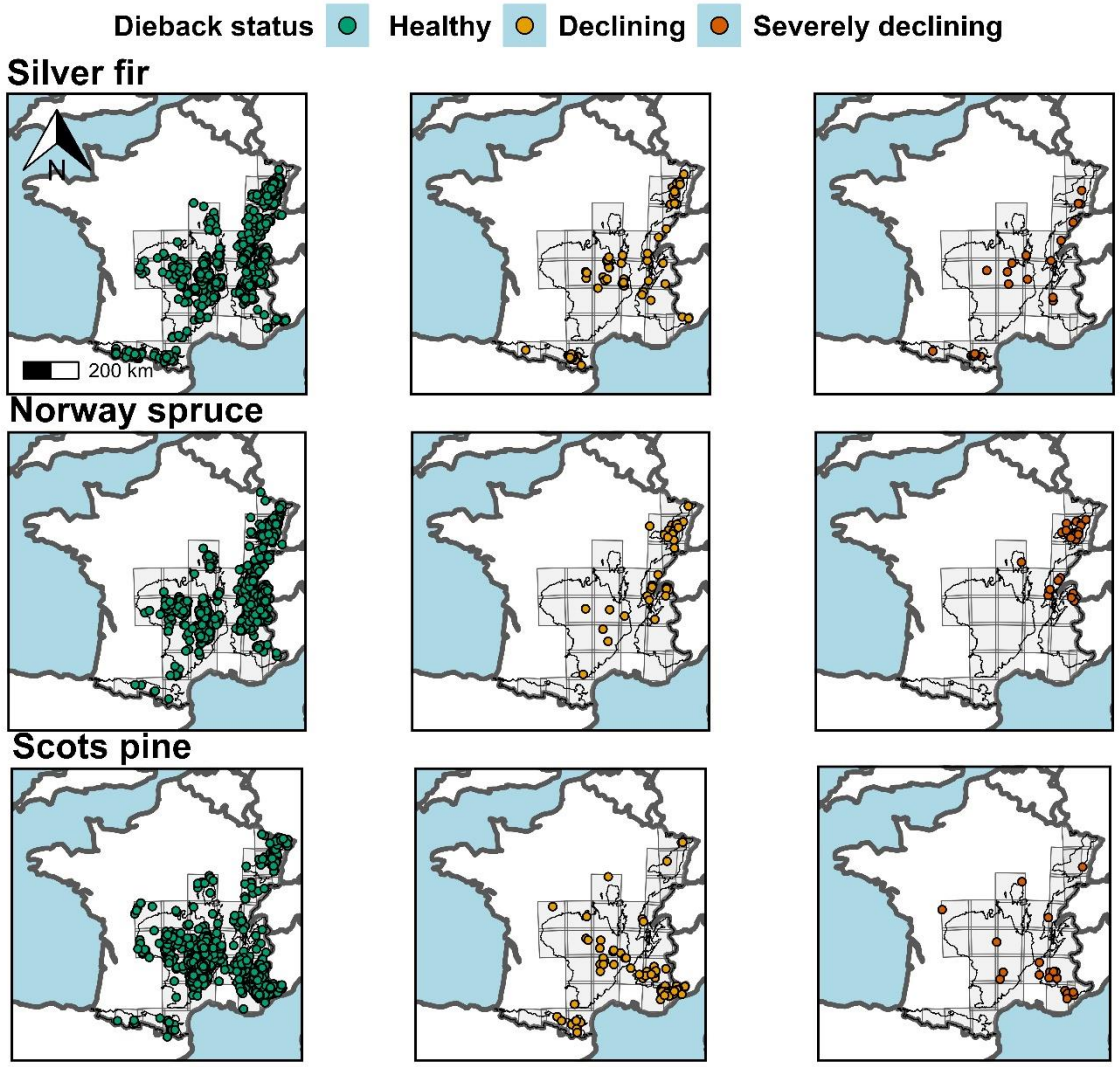

Fig.1: Distribution of the 1,964 study plots located in the selected mountain ranges, by species and dieback status. The location of the selected Sentinel-2 tiles is delineated in grey (each tile contains at least 100 ground observations) (Dieback status categories correspond to [0%-25%],]25% - 50%] and]50% - 100%] for "Healthy", "Declining" and "Severely declining" respectively).

The NFI database provided information on the social status of living trees (whether dominant or co-dominant), but not dead ones. Instead, the ratio of a tree's circumference to the mean circumference of all the trees in the plot was used to identify dominant and co-dominant trees for dead trees. This threshold was calibrated for each species (Tab.A.1). As dieback was not

assessed for the small trees, we eliminated the plots where more than 50% of the trees had a diameter at breast height of less than 22.5 cm.

On 55% of the plots, we used the percentage of dead branches (DB) and leaf defoliation (LD) to determine the degree of dieback for each of the dominant and co-dominant trees (Goudet et al., 2018). As LD was not available, we only used DB for the remaining 45%. A DB value of 100% indicates a dead tree. When both DB and LD were assessed, we calculated the *Idx* index (Eq. 1), as recommended by the French Forest Health Service (DSF): When LD was missing, the *Idx* index took DB alone.

$$Idx = DB + (1 - DB/100) * LD \quad \text{Eq.1}$$

For the dataset studied, silver fir, Norway spruce and Scots pine had mortality rates of 3.0%, 5.0% and 6.1%, respectively. These rates are higher than those observed in France from 2009 to 2015 (Taccoen, 2019). At the plot level, dieback was calculated for each species by weighting the individual scores of the dominant or co-dominant trees according to the proportion of their species in the total basal area of the plot. To describe the health status of each species in the plot, we attributed a species dieback plot score (*Dps*) ranging from 0 % (healthy) to 100 % (all the trees of the species are dead), as follows:

$$Dps = \sum_{i=1}^{n} Idx * Gi/Gp \quad \text{Eq. 2}$$

where, for the considered species, *Gi* is individual tree basal area, n total number of trees, and *Gp* plot basal area.

The plots were then divided into two groups: 862 pure stands, in which the species covered 100% of the basal area of the dominant-codominant tree layer of the plot, and 1,102 mixed

196 stands, in which the target species covered less than 100% of the basal area (Fig.2). In the
197 mixed stands, only the plots with healthy non-target species were retained.

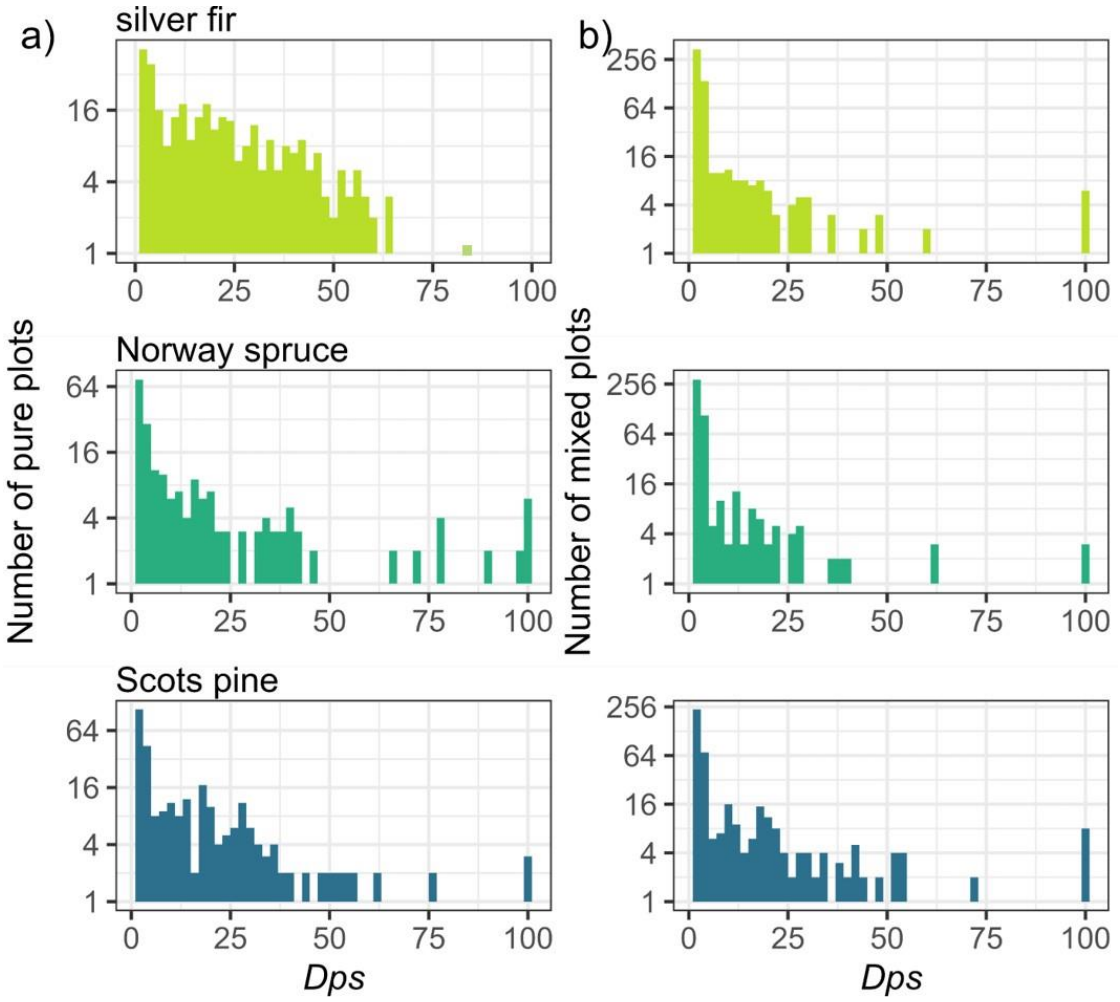

198

199 *Fig.2: Log2 transformed distribution of the species dieback plot score (Dps) in a) pure*
200 *(N=862), and b) mixed (N=1,102) stands for each studied species.*
201

202 *Satellite data*

203

204 We used satellite-image time series (SITS) acquired by Sentinel-2A and 2B which is part of the
205 Copernicus program (Drusch et al., 2012). Revisit time is five days and sensors acquire
206 information in 13 spectral bands, ten of which are available with atmospheric correction. The
207 spectral bands cover the VIS, NIR and SWIR domains. The spectral characteristics (centre
208 wavelength for each band) and spatial resolution are given in Table.A.1.

The Sentinel-2 Level-2A images for the 28 Sentinel-2 tiles covering the study area (Fig.1), pre-processed for atmospheric correction by the MAJA processing chain, were downloaded from the Theia platform1 for the period from January 1, 2016 to December 31, 2023. Acquisitions with more than 30% cloud cover were discarded, resulting in 1,186 images and a revisit time ranging from six to 19 days. Non-valid observations corresponding to unmasked clouds, haze and snow were removed based on a reflectance threshold on band (B2) excluding surface reflectance > 6% out of the physical range (0-1), according to the method developed by Dutrieux et al. (2021). A pixel was attached to a plot if its centroid was included in the plot area resulting in an array from four to 100 pixels per plot (mean = 9 pixels, standard deviation = 3 pixels). The *Dps* defined at the plot level was then applied to each of its pixels. For each image associated with each plot, the plot was retained if the spectral information was valid (no clouds or shadows) in at least 50% of its pixels. We selected eight vegetation indices regularly used in conifer dieback detection studies and weakly intercorrelated (Tab.1, Fig.A.2): CRSWIR, NDWI, NDVI, REP, IRECI, CRRE, NDMI and MCARI (Table.1).

Table 1: Presentation of the selected vegetation indices. λBi and Bi are, respectively, the wavelength and reflectance (nm) of band i (Tab.A.1).

Vegetation index	Formulation	Reference
CR_{SWIR}	B11/ ((B8A + (λ_{B11} - λ_{B8A}) * ((B12-B8A) / (λ_{B12}- λ_{B8A})))	(Dutrieux et al., 2021)
NDWI	(B3-B8)/(B3+B8)	(McFeeters, 1996)
NDVI	(B8-B4)/(B8+B4)	(Tucker, 1979)
REP	700+35*(((B4+B7)/2)-B5)/(B6-B5)	(Gitelson & Merzlyak, 1998)
IRECI	(B7-B4)/(B5/B6)	(Frampton et al., 2013)
CR_{RE}	B5/(B4+(λ_{B5}- λ_{B4})*(B6-B4)/(λ_{B6}- λ_{B4}))	(Huang et al., 2004)
MCARI	((B5-B4)-0.2*(B5-B3))*(B5/B4)	(Daughtry, 2000)

NDMI	(B8A-B11)/(B8A+B11)	(Vogelmann & Rock, 1988)

Time-series analysis

FORDEAD approach

The FORDEAD time-series approach (Dutrieux et al., 2021) is an anomaly detection method applicable to satellite-image time series that operates at the pixel level. FORDEAD assumes that the seasonality of spectral information is stable over time for 'healthy' forest pixels. Spectral information may correspond to a vegetation index or to a spectral band, depending on the vegetation property expected to change with dieback. For each pixel, the seasonality corresponding to the healthy stage is calibrated with a harmonic model fitted over a sufficiently long period and based on a least-squares criterion (Eq.3). Anomalies correspond to a deviation from the harmonic model when extrapolated over time (Fig. 4). The training period defined to fit the harmonic model should be long enough to cover at least one full growing season, with a sufficient number of acquisitions. Here, we used a training period of two years (2016 and 2017) during which very little dieback occurred (Fig.A.3). Two growing seasons during the two-year training period were considered when fitting the harmonic model in order to account for within - and between-season variability (Rautiainen et al., 2018). A minimum of ten Sentinel-2 images with at least one per season during the training period were required to calibrate the model for each pixel, and the plot was only retained if at least 50% of its pixels could be calibrated. The most extreme 5% of the reflectance values for each spectral band (2.5% lowest and 2.5% highest) were eliminated during the training period in order to improve model fit.

$$HM = a1 + b1*\sin(2\pi t/T) + b2*\cos(2\pi t/T) + b3*\sin(4\pi t/T) + b4*\cos(4\pi t/T) \quad \text{, Eq. 3}$$

where T=365.25, t = number of days between the Sentinel-2 image and 01/01/2015, and (*a1*,*b1*,*b2*,*b3*,*b4*) are pixel model coefficients.

After the training period, for every Sentinel-2 image available for the period 2018-2023, a spectral anomaly at the plot level was defined as the average difference between the current value of the spectral index and the value predicted by the harmonic model for each pixel (Lastovicka et al. 2020) (blue arrows in Fig.3). The anomalies were then averaged over different time periods, called integration periods (orange arrows in Fig.3).

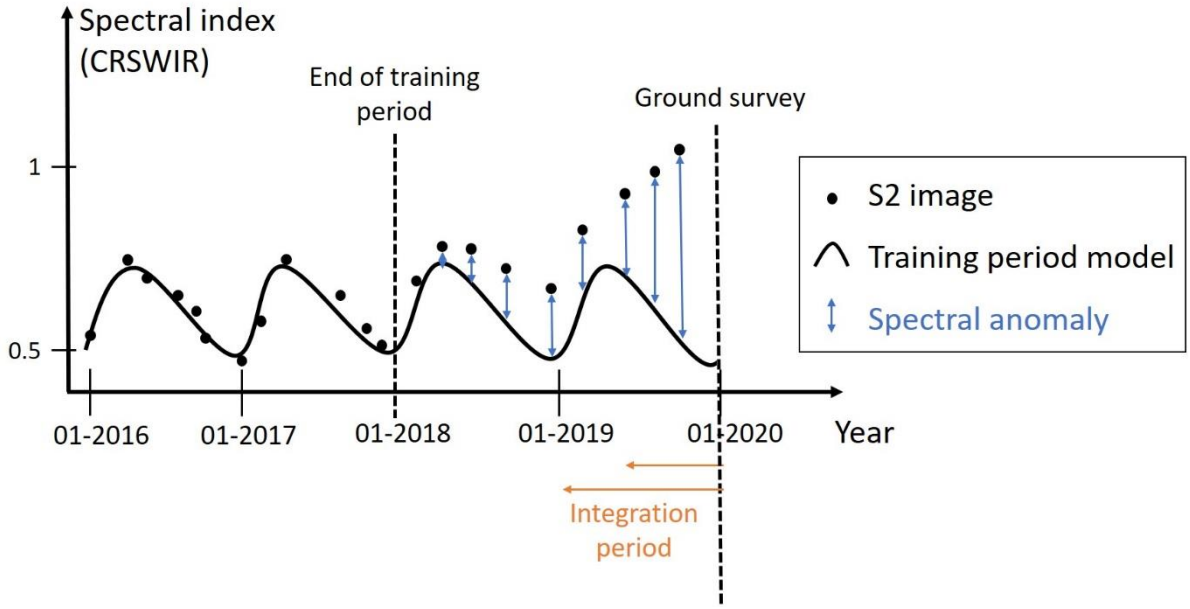

Fig.3: Schematic pixel trajectory analysed with the FORDEAD method.
The figure above shows CRSWIR dynamics for a plot with dieback symptoms observed in 01/2020.

After applying the above filters to the dataset, the 18 spectral indices (eight vegetation indices and ten Sentinel-2 spectral bands) were calculated for 1,691 of the 1,964 plots available. This represented 742 pure stands (289, 166 and 287 for silver fir, Norway spruce and Scots pine, respectively) and 949 mixed stands (438, 339 and 392 with silver fir, Norway spruce and Scots pine, respectively, including possible mixtures with each other).

Capacity of spectral indices and anomaly integration periods to predict dieback

For each of the 18 spectral indices, we used the averaged spectral anomaly as a predictive value for species *Dps* for the pure plots. Several integration periods, from one to 40 months, of the spectral anomaly were tested for each spectral index. We fitted a linear regression model with a quadratic term composed of the average observed anomaly for each spectral index over each anomaly's integration period as the y variable, and the *Dps* as the x variable, then calculated the coefficient of determination (R^2). For each species, we selected the best spectral index and integration period that, in combination, best correlated with the actual measured dieback. We then evaluated its capacity to detect dieback gradients for different degrees of mixture (Tab.A.3). We evaluated the quality of the model by looking at its coefficient of determination (R^2) and root mean square error (RMSE) (Chai & Draxler, 2014; Figueiredo Filho et al., 2011).

In order to compare our results with a more classical approach, contrasting the healthy and degraded condition of the trees, we classified the pure plots into two classes from the 30% *Dps* threshold recommended by the French Forest Health Service. For each species, this binary status was modelled using the best spectral index and integration period with a generalised linear regression model. A Receiver Operating Characteristic (ROC) curve was used to determine when each plot should be considered either healthy or declining (Fielding & Bell, 1997). Standard metrics overall accuracy (OA) and balanced accuracy (BA) (Pedregosa et al., 2011) were calculated (Fig.A.4). OA estimates the percentage of well classified plots and BA is defined as the average between the true positive rate and the true negative rate and is not influenced by an unbalanced dataset. The performance was validated with repeated tenfold stratified cross-validation; 70% of the dataset was used for training and the remaining 30% for testing.

Results

Performance of spectral indices and integration periods varies among conifer species

The performance of the spectral indices in predicting dieback gradients varied greatly among species (Fig.4). The best performing model had an R^2 of 0.54 for Norway spruce, 0.34 for silver fir, and 0.16 for Scots pine (RMSE 24, 22 and 22%, respectively). When considering only healthy and declining plots, OA and BA were 77% and 74% for Norway spruce, 61% and 63% for silver fir, and 64% and 62% for Scots pine (Tab.A.4).

The spectral index with the highest performance differed among species: IRECI for silver fir, CRSWIR for Norway spruce and CRRE for Scots pine. The performances were strongly species-dependent. For example, IRECI, the most efficient spectral index for silver fir, had an R^2 37% lower than CRSWIR for Norway spruce (28% RMSE) and 13% lower than CRRE for Scots pine (22% RMSE). CRSWIR was the best spectral predictor of the dieback gradient in terms of average R^2 regardless of species. However, selecting CRSWIR for all three species would have had a major impact on dieback predictability. The R^2 value for silver fir dieback predictions would have decreased from 0.34 to 0.19 (24% RMSE) and the capacity to predict Scots pine gradient of dieback would have been negligible (22% RMSE).

With the best spectral index applied for each species, optimal anomaly integration periods were 15 months for silver fir, four months for Scots pine and one month for Norway spruce (Fig. 5a). The best integration period in terms of average R^2 was nine months regardless of species. Applying a nine-month integration period for all three species, would have had a slight impact on the predictability of dieback. The R^2 value for silver fir, Norway spruce and Scots pine dieback predictions would have decreased by 6%, 7% and 19%, respectively.

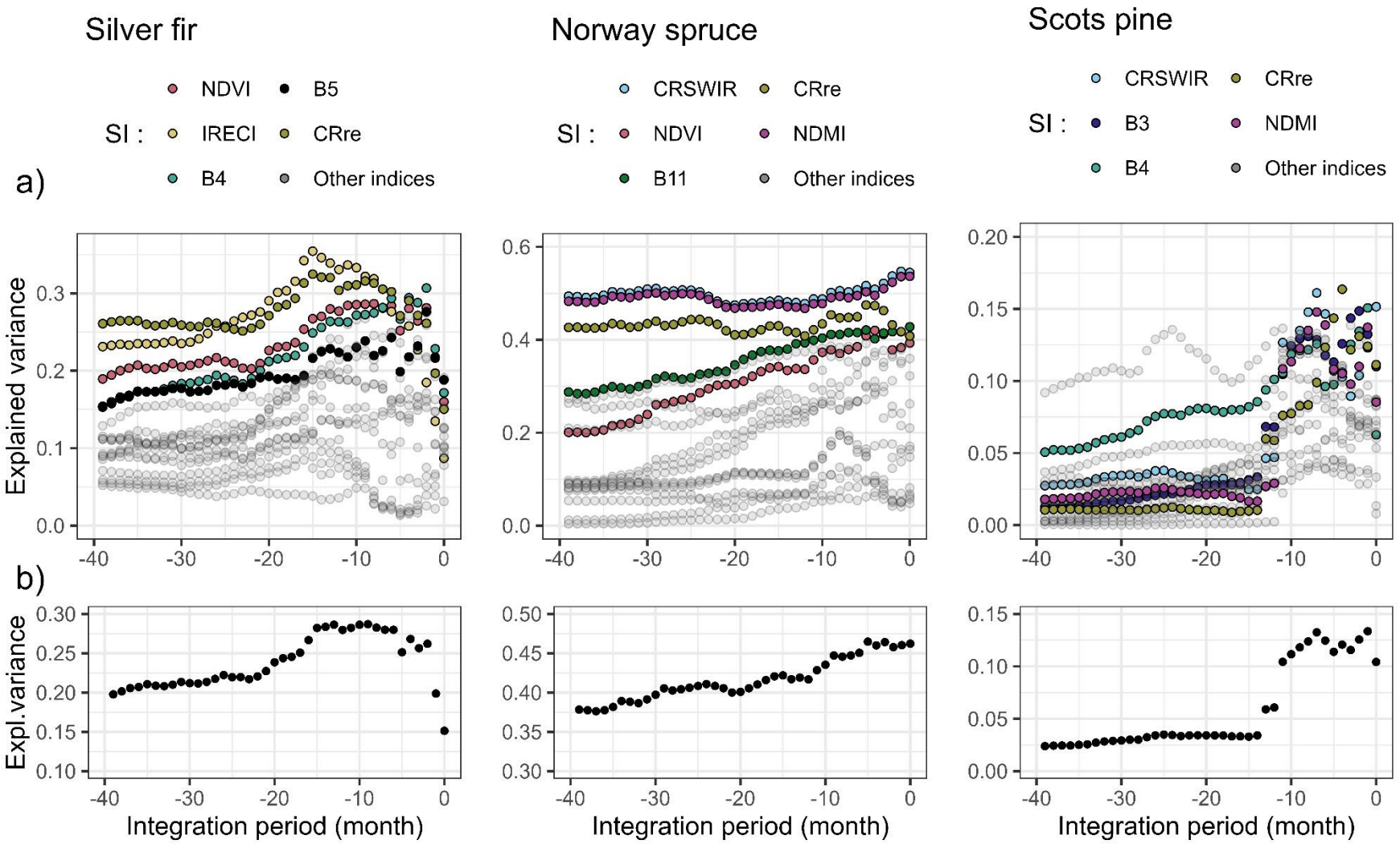

Fig.4: a) Explained variance (R^2) of different spectral index (SI) anomalies in detecting a continuous dieback gradient for silver fir, Norway spruce and Scots pine (n =289,166 and 287, respectively), for a range of integration periods. The five SIs with the highest explained variance is represented in colour. b) R^2 of the five best spectral indices averaged for each period. Each dot represents the R^2 between the Dps and the spectral anomaly for one SF and integration period.

Dieback detection according to dieback intensity and mixture percentage

We selected the spectral index and integration period that best predicted the observed dieback gradients for pure stands and examined its response to varying degrees of mixture. The spectral anomalies differed according to species, dieback intensity and mixture proportion (Fig.5). In pure stands, the spectral anomalies of silver fir showed a linear response to increasing dieback values. For Norway spruce, the response was exponential, while for Scots pine, the regression line was almost horizontal. Differences from healthy stands appeared from a *Dps* of 20-30% for silver fir, in contrast to Scots pine for which a high level of dieback was required to distinguish healthy from declining plots. For Norway spruce, no real distinction was discernible before a 50% *Dps* in pure stands, but beyond that value, the difference became increasingly accentuated.

Dieback detection was more challenging for species in mixed stands. However, the degree of mixing from which dieback can be detected varied among species. Even with the best spectral index, it was difficult to detect dieback for Norway spruce or Scots pine in mixed stands, whereas it was possible for silver fir, particularly when the species exceeded 50 % of the total basal area of the stand. The four next best spectral indices (Fig.4) showed similar patterns.

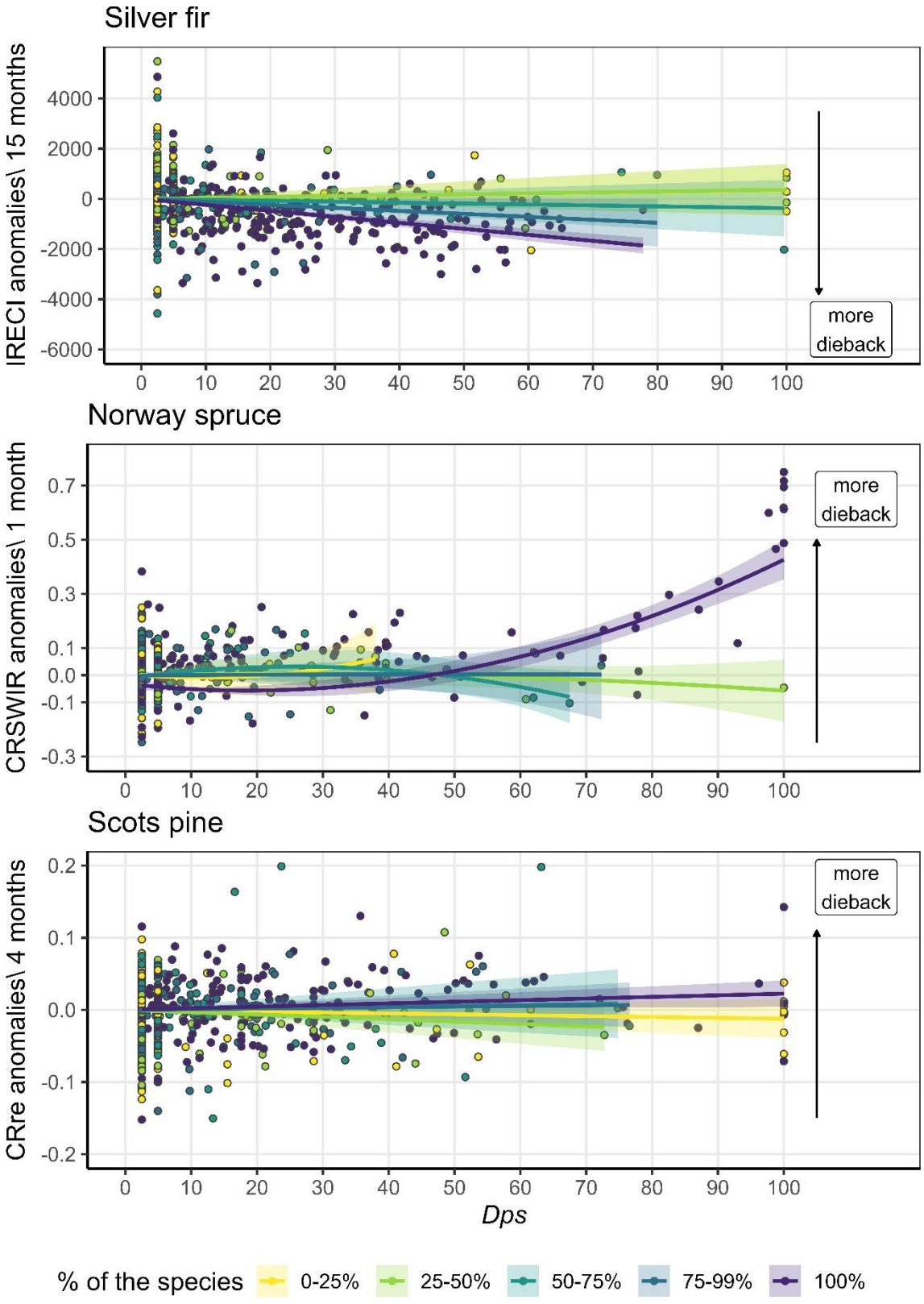

Fig.5: Comparison between spectral index anomalies and dieback gradient (Dps) for pure stands (noted 100 %) and different mixture classes for silver fir, Norway spruce and Scots pine (n=727,505 and 679 respectively). The dots represent each plot's averaged spectral anomalies. The supposed evolution of the spectral index under dieback is indicated by the black arrow. The regression curves are fitted and 95% confidence intervals are represented. R^2 and RMSE values are in Tab.A.5.

Discussion

The most efficient spectral index varied by species

Although a similar method is often used to detect dieback for different species (Lambert et al., 2013; Senf et al., 2018), we found predictions can be improved at the species level. This suggests that species-specific physiological responses are at play (Garrity et al., 2013). The differences among species may also be explained by the factors causing the dieback, which induce different symptoms. Silver fir and Scots pine dieback were most accurately identified with, respectively, IRECI and CRRE. Both indices contain visible and red-edge bands, which appear to be relevant for monitoring dieback in both species (Hawryło et al., 2018). This suggests that the detection of their dieback may depend on changes in photosynthetic activity, particularly chlorophyll content, which is the main factor influencing the reflectance of vegetation in the visible and red-edge regions. For these two species, the factors are more diverse than for Norway spruce but an increasing amount of the dieback reported by the French Forest Health Service is associated with the fungus Sphaeropsis sapinea for Scots pine (Fabre et al., 2011), and with the bark beetle Pitokteines spp. for silver fir (Durand-Gillmann et al., 2014), both of which cause crown discolouration. This is consistent with spectral index related to changes in chlorophyl content performing the best.

Norway spruce dieback was optimally detected with CRSWIR, which takes advantage of NIR and SWIR reflectance (Fig.A.5). This spectral index was developed specifically to detect Norway spruce dieback, and was identified as the most relevant spectral index during the development of the FORDEAD method (Dutrieux et al., 2021). In contrast to silver fir and Scots pine, bark beetles, especially Ips typographus L., are an important factor in Norway spruce dieback. They initially affect the water content of the tree crown by forcing the stomata to close (Abdullah et al., 2019b), thereby reducing their photosynthetic activity (Kautz et al.,

2023). This explains the high performance of CRSWIR, which is correlated with canopy water content and therefore particularly relevant for detecting bark beetle infestations (Abdullah et al., 2019a). Using the same spectral index to predict dieback for all species decreased detection performance, especially for silver fir, thus illustrating the benefit of detecting dieback at the species level. For all species, spectral bands were less effective than vegetation indices, thus confirming the latter's interest (Abdullah et al., 2019a).

Detection accuracy varies among species

Time-series analysis varied in performance among the studied coniferous species, with much better dieback gradient detection for Norway spruce than for silver fir or Scots pine. Differences in dieback detection for species belonging to the same functional group have rarely been investigated but similar observations have already been reported in studies conducted at the local scale with high-resolution unmanned aerial systems (Ecke et al., 2024; Kamińska et al., 2018). These differences may be explained by variations in the spectral characteristics of declining plots for each species, or by local mortality patterns, canopy cover or causes of dieback. The influence of the understory on surface reflectance measured with Sentinel-2 may be particularly important in severely declining plots with limited vegetation cover (Meiforth et al., 2020). Pine forest canopies are less dense than those of spruce or fir forests (Grabska & Socha, 2021); this could explain the lower detection rate for Scots pine dieback. When the influence of the understory is limited, as it is on poor sandy soils, performance can be better (Hawryło et al., 2018). These results highlight the importance of considering species-specific characteristics to improve large-area monitoring. Despite the limited number of studies focusing on dieback gradients at the species level, our performance appears to be in line with other studies. For example, Lambert (2013) reported 31 % of explained variance in detecting

388 the proportion of stressed silver fir trees using NDVI time series analysis. Crespo-Antia et al.,
389 (2024) found a correlation of -0.57 between silver fir stand defoliation and Enhanced
390 Vegetation Index (EVI) time-series. Most existing studies focus on classifying a binary variable
391 representing the presence or absence of dieback, which also showed close performance
392 (Abdullah et al., 2019b; Bárta et al., 2021). For example, Bárta et al., (2021) obtained an OA
393 of 78% for discriminating healthy from declining Norway spruce pure stands through time
394 series analysis in Central Europe. Grabska et al., (2020) obtained an OA of 75% detecting
395 dominated Scots pine forest loss with Sentinel-2 time series in Poland. Our results were
396 obtained even though dead branches and defoliation are more difficult to detect than stand
397 changes in colour or defoliation alone, as is the case in most studies (Abdullah et al., 2019a;
398 Meneghini et al., 2022). We highlighted a non-linear response for Norway spruce with severe
399 symptoms. Meddens et al., (2013), who examined changes in dieback accuracy as a function of
400 red-stage percentage within pixels for Norway spruce, observed a similar result. We did not
401 find the same nonlinearity for silver fir and Scots pine, possibly due to the absence of stands
402 with high levels of dieback in our sample (maximum dieback plot score of 78% in silver fir
403 stands, and only seven plots with a plot dieback score above 70% for Scots pine stands).
404 Collecting a large number of ground observations with equal representation of dieback stages
405 is challenging due to the rarity of declining stands and the frequent harvesting of declining trees.
406 To mitigate this problem, we added plots located in areas of significant dieback to the
407 systematic sampling plots from the NFI. The differences in dieback intensity observed at the
408 plot scale also reflect different patterns among the three species studied. In the declining NFI
409 plots, we observed a higher mortality rate for Norway spruce (39%), which is experiencing
410 more massive dieback, than for Scots pine (26%) and silver fir (23%). These results suggest
411 that the potential for mapping dieback areas is better for Norway spruce than for silver fir or
412 Scots pine.

Shorter integration period for Norway spruce than for Scots pine and silver fir

The optimal integration period for Norway spruce dieback was one month before field observations, while for the other two species, a much longer period must be considered. This is consistent with Bárta et al. (2021), who showed that the trajectories of vegetation indices for red-stage Norway spruce stands deviated from their usual trend one or two months before field observations. For silver fir, on the other hand, Lambert et al. (2013) found the highest performance when considering spectral anomalies one or two years before field observations. The way different species react over time is linked to the cause of the stress. For example, Cailleret et al., (2017) studied tree growth prior to mortality and showed a shorter dieback period when mortality was caused by a biotic agent - particularly bark beetles - compared to a climatic cause. Norway spruce dieback is closely linked to bark beetle infestations, whereas for the other two species, decline is more common due to non-biotic factors and biotic factors are less aggressive (DSF & IGN, 2024). This could explain the earlier detection of anomalies for Norway spruce compared to Scots pine and silver fir.

Detection of the early-warning stage and dieback in mixtures remains challenging

The ability to detect early symptoms of dieback would allow managers to better anticipate crises and adapt forest management planning (Torres et al., 2021). Detecting gradients, including the early-warning stage, is complex, as demonstrated by White et al., (2005) and Meddens et al., (2013), whose results showed low accuracy at early dieback stages in conifer forests. In our study, we did not detect any early signals for Norway spruce dieback in pure stands. However, we did identify early signals for silver fir, and to a lesser extent for Scots pine, despite poorly estimated dieback gradients. These results suggest that early-warning dieback stages cannot be

detected for all species. This could hinder effective management of bark beetle infestations for Norway spruce, for example.

Seventy percent of European forests are mixed (UNECE & FAO, 2011). Even so, most studies assessing forest dieback through satellite detection have focused on pure stands (Marx & Kleinschmit, 2017), or have not considered the influence of species mixture when studying dieback for a given species (Hawryło et al., 2018). As expected, the detection of dieback performed less well in mixtures as the proportion of healthy species increased. At intermediate levels of mixture, we were better able to detect dieback for silver fir than for Scots pine and, especially, Norway spruce, for which dieback detection was efficient only in pure stands. For Scots pine and Norway spruce, the absence of mixed stands with high levels of dieback (plot dieback score > 70%) limited the comparison with pure stands. Mixtures - particularly between deciduous and coniferous trees - clearly increase the complexity of dieback detection (Lee & Lee, 2019). In our study, deciduous species were present in 72% of the mixed stands. With field survey information on species at the pixel scale rather than at the plot scale, the description of plot heterogeneity and the accuracy of dieback monitoring should improve. Precise species distribution maps are needed to adapt time-series analyses to the stand's composition. Some promising novel methods of species identification based on satellite time series or artificial intelligence are in development and may allow researchers to produce updated maps of species distribution over broad areas (Hermosilla et al., 2022; Gilles et al., 2024).

Uncertainties and improvements

The forest plots we studied covered a wide range of environmental conditions across Europe, in terms of altitude, soil, climate and management. Despite the pixel-scale calibration of our time-series analysis, which we expected would account for the local context (forest type, stand

characteristics, elevation), sources of uncertainty remain that can be due to local disturbances caused by changes in vegetation cover or management. We know that tree mortality increased In France after our calibration period (2016-2017) but we cannot be sure that no dieback occurred during the training period (DSF & IGN, 2024). We may therefore have underestimated mortality in some plots. The more time that elapses after the training period, the greater the risk of confounding mortality with changes related to stand dynamics or management. One solution might be to calibrate the model to a moving window (Mouret et al., 2024), but in this case, care should be taken to avoid calibrating the model during a period of higher mortality.

Finally, we considered the dieback plot score to be uniform at the plot scale and this probably limited the model's performance since the actual distribution of declining trees was not uniform throughout the plot, particularly for silver fir and Scots pine. Further analyses should evaluate the interest of integrating tree location inside the plot, for example, by using sensors with higher resolutions (airborne, UAV...) to allow work at the pixel scale and not at the plot scale.

The above-mentioned limitations can be important since they introduce noise into the spectral anomaly signals (Grabska & Socha, 2021). However, these uncertainties would not have affected the differences among the species highlighted in this paper.

Finally, the time series analysis method we used is based on the detection of anomalies with a single index. For all three species, we found different responses related to dieback intensity in almost all the spectral bands, which cannot be represented by a single vegetation index. The method could therefore be further optimised by combining different spectral indices, a technique that has been identified as a vector for improving current satellite-based forest monitoring (Ye et al., 2021). It should be noted, however, that this technique does not systematically improve the accuracy of dieback detection (Mouret et al., 2024).

Conclusion

We reveal important among-species differences in performance, spectral indices, anomaly integration periods, early warning stages and dieback detection. The ability of remote sensing to detect declining stands is related to dieback causes and patterns, which are different depending on the species and are also strongly influenced by mixture. Our results argue in favour of calibrating detection methods at the species level rather than at the functional group level. Our research should be extended to the other major tree species to determine the best parameters to assess and monitor their dieback. Our results also illustrate the interest of analysing Sentinel-2 time series, which could be used to produce high-resolution dieback maps at the species level when accurate and detailed land-use maps are available. This would make it possible to monitor dieback trends over time. Dieback is increasing in many parts of the world and there is an urgent need to develop an efficient monitoring system that provides a periodic picture of forest health and can help to improve forest management planning and policy making over large areas.

Acknowledgment

This work was supported by the French National Research Agency through the Laboratory of Excellence ARBRE (ANR-12- LABXARBRE-01).

We are thankful for access to forest inventory data in France (NFI, CNPF, ONF, DSF, AgroParisTech) and to our SILVA and AgroParisTech colleagues for their support.

Declaration of interest statement

The author(s) declare that they have no known competing financial interests or personal relationships that could have appeared to influence the work reported in this paper.

Author contributions: CRediT

Jean-Claude Gégout: Conceptualization, Methodology, Writing - Review & Editing, Supervision, **Raphael Dutrieux:** Methodology, Software, Data Curation, **Jean-Baptiste Féret:** Conceptualization, Methodology, Software, Writing - Review & Editing, Data Curation, **Cédric Vega:** Conceptualization, Methodology, Resources, Writing - Review & Editing, **Thierry Belouard:** Conceptualization, Methodology, Resources, Writing - Review & Editing, **Anne Jolly:** Conceptualization, Methodology, Resources, Writing - Review & Editing, **Juliette Cansell:** Resources, Writing - Review & Editing, **Christian Piedallu:** Conceptualization, Methodology, Resources, Writing - Review & Editing, Supervision, Funding acquisition, Project administration

References

Abdullah, H., Skidmore, A. K., Darvishzadeh, R., & Heurich, M. (2019a). Sentinel-2 accurately maps green-attack stage of European spruce bark beetle (*Ips typographus* , L.) compared with Landsat-8. *Remote Sensing in Ecology and Conservation*, *5*(1), 87–106. https://doi.org/10.1002/rse2.93

Abdullah, H., Skidmore, A. K., Darvishzadeh, R., & Heurich, M. (2019b). Timing of red-edge and shortwave infrared reflectance critical for early stress detection induced by bark beetle (Ips typographus, L.) attack. *International Journal of Applied Earth Observation and Geoinformation*, *82*, 101900. https://doi.org/10.1016/j.jag.2019.101900

Allen, C. D. (2009). *Climate-induced forest dieback: An escalating global phenomenon? 60*.

Bárta, V., Lukeš, P., & Homolová, L. (2021). Early detection of bark beetle infestation in Norway spruce forests of Central Europe using Sentinel-2. *International Journal of*

Applied Earth Observation and Geoinformation, *100*, 102335. https://doi.org/10.1016/j.jag.2021.102335

Bontemps, J.-D., Hervé, J.-C., & Denardou, A. (2019). Partition idéalisée et régionalisée de la composition en espèces ligneuses des forêts françaises. *Écoscience*, *26*(4), 291–308. https://doi.org/10.1080/11956860.2019.1588511

Cailleret, M., Jansen, S., Robert, E. M. R., Desoto, L., Aakala, T., Antos, J. A., Beikircher, B., Bigler, C., Bugmann, H., Caccianiga, M., Čada, V., Camarero, J. J., Cherubini, P., Cochard, H., Coyea, M. R., Čufar, K., Das, A. J., Davi, H., Delzon, S., … Martínez-Vilalta, J. (2017). A synthesis of radial growth patterns preceding tree mortality. *Global Change Biology*, *23*(4), 1675–1690. https://doi.org/10.1111/gcb.13535

Carter, G. A., & Knapp, A. K. (2001). Leaf optical properties in higher plants: Linking spectral characteristics to stress and chlorophyll concentration. *American Journal of Botany*, *88*(4), 677–684. https://doi.org/10.2307/2657068

Chai, T., & Draxler, R. R. (2014). Root mean square error (RMSE) or mean absolute error (MAE)? – Arguments against avoiding RMSE in the literature. *Geoscientific Model Development*, *7*(3), 1247–1250. https://doi.org/10.5194/gmd-7-1247-2014

Chen, S., Woodcock, C. E., Bullock, E. L., Arévalo, P., Torchinava, P., Peng, S., & Olofsson, P. (2021). Monitoring temperate forest degradation on Google Earth Engine using Landsat time series analysis. *Remote Sensing of Environment*, *265*, 112648. https://doi.org/10.1016/j.rse.2021.112648

Crespo-Antia, J. P., Gazol, A., Pizarro, M., González de Andrés, E., Valeriano, C., Rubio Cuadrado, Á., Linares, J. C., & Camarero, J. J. (2024). Matching Vegetation Indices and Tree Vigor in Pyrenean Silver Fir Stands. *Remote Sensing*, *16*(23), 4564. https://doi.org/10.3390/rs16234564

559 Drechsel, J., & Forkel, M. (2025). Remote sensing forest health assessment – a
560 comprehensive literature review on a European level. *Central European Forestry*
561 *Journal*, *71*(1), 14–39. https://doi.org/10.2478/forj-2024-0022
562 Drusch, M., Del Bello, U., Carlier, S., Colin, O., Fernandez, V., Gascon, F., Hoersch, B.,
563 Isola, C., Laberinti, P., Martimort, P., Meygret, A., Spoto, F., Sy, O., Marchese, F., &
564 Bargellini, P. (2012). Sentinel-2: ESA's Optical High-Resolution Mission for GMES
565 Operational Services. *Remote Sensing of Environment*, *120*, 25–36.
566 https://doi.org/10.1016/j.rse.2011.11.026
567 DSF, & IGN. (2024, January). *Etat dégradé des forêts de France: Proposition d'une*
568 *méthodologie d'estimation des surfaces concernées*. https://agriculture.gouv.fr/bilans-
569 annuels-en-sante-des-forets
570 Durand-Gillmann, M., Cailleret, M., Boivin, T., Nageleisen, L.-M., & Davi, H. (2014).
571 Individual vulnerability factors of Silver fir (Abies alba Mill.) to parasitism by two
572 contrasting biotic agents: Mistletoe (Viscum album L. ssp. abietis) and bark beetles
573 (Coleoptera: Curculionidae: Scolytinae) during a decline process. *Annals of Forest*
574 *Science*, *71*(6), 659–673. https://doi.org/10.1007/s13595-012-0251-y
575 Dutrieux, R., FERET, J.-B., OSE, K., & DE BOISSIEU, F. (2021). *Package Fordead*
576 [Dataset]. [object Object]. https://doi.org/10.15454/4TEO6H
577 Ecke, S., Stehr, F., Frey, J., Tiede, D., Dempewolf, J., Klemmt, H.-J., Endres, E., & Seifert, T.
578 (2024). Towards operational UAV-based forest health monitoring: Species
579 identification and crown condition assessment by means of deep learning. *Computers*
580 *and Electronics in Agriculture*, *219*, 108785.
581 https://doi.org/10.1016/j.compag.2024.108785
582 *Évaluation des ressources forestières mondiales 2020*. (2021). FAO.
583 https://doi.org/10.4060/ca9825fr

584 Fabre, B., Piou, D., Desprez-Loustau, M., & Marçais, B. (2011). Can the emergence of pine
585 *Diplodia* shoot blight in France be explained by changes in pathogen pressure linked
586 to climate change? *Global Change Biology*, *17*(10), 3218–3227.
587 https://doi.org/10.1111/j.1365-2486.2011.02428.x
588 Fielding, A. H., & Bell, J. F. (1997). A review of methods for the assessment of prediction
589 errors in conservation presence/absence models. *Environmental Conservation*, *24*(1),
590 38–49. https://doi.org/10.1017/S0376892997000088
591 Figueiredo Filho, D. B., Silva Júnior, J. A., & Rocha, E. C. (2011). What is R2 all about?
592 *Leviathan (São Paulo)*, *3*, 60. https://doi.org/10.11606/issn.2237-
593 4485.lev.2011.132282
594 Frampton, W. J., Dash, J., Watmough, G., & Milton, E. J. (2013). Evaluating the capabilities
595 of Sentinel-2 for quantitative estimation of biophysical variables in vegetation. *ISPRS*
596 *Journal of Photogrammetry and Remote Sensing*, *82*, 83–92.
597 https://doi.org/10.1016/j.isprsjprs.2013.04.007
598 Gallardo-Salazar, J. L., Sáenz-Romero, C., Lindig-Cisneros, R., López-Toledo, L., Blanco-
599 García, J. A., & Endara-Agramont, Á. R. (2023). Three decades of remote sensing
600 analysis of forest decline related to climate change: A bibliometric study. *Cuadernos*
601 *de Investigación Geográfica*, *49*(1), 69–87. https://doi.org/10.18172/cig.5639
602 Garrity, S. R., Allen, C. D., Brumby, S. P., Gangodagamage, C., McDowell, N. G., & Cai, D.
603 M. (2013). Quantifying tree mortality in a mixed species woodland using
604 multitemporal high spatial resolution satellite imagery. *Remote Sensing of*
605 *Environment*, *129*, 54–65. https://doi.org/10.1016/j.rse.2012.10.029
606 Gilles, A., Jonathan, L., Juliette, C., Nicolas, L., Christian, P., & Hugues, C. (2024). Spatial
607 and remote sensing monitoring shows the end of the bark beetle outbreak on Belgian

608 and north-eastern France Norway spruce (Picea abies) stands. *Environmental*
609 *Monitoring and Assessment*, *196*(3), 226. https://doi.org/10.1007/s10661-024-12372-0
610 Gitelson, A. A., & Merzlyak, M. N. (1998). Remote sensing of chlorophyll concentration in
611 higher plant leaves. *Advances in Space Research*, *22*(5), 689–692.
612 https://doi.org/10.1016/S0273-1177(97)01133-2
613 Goudet, M., Saintonge, F.-X., & Nageleisen, L.-M. (2018). *Quantifier l'état de santé de la*
614 *forêt, méthode simplifiée d'évaluation*. https: //agriculture.gouv.fr/telecharger/90879
615 Grabska, E., Hawryło, P., & Socha, J. (2020). Continuous Detection of Small-Scale Changes
616 in Scots Pine Dominated Stands Using Dense Sentinel-2 Time Series. *Remote Sensing*,
617 *12*(8), 1298. https://doi.org/10.3390/rs12081298
618 Grabska, E., & Socha, J. (2021). Evaluating the effect of stand properties and site conditions
619 on the forest reflectance from Sentinel-2 time series. *PLOS ONE*, *16*(3), e0248459.
620 https://doi.org/10.1371/journal.pone.0248459
621 Hartmann, H., Schuldt, B., Sanders, T. G. M., Macinnis-Ng, C., Boehmer, H. J., Allen, C. D.,
622 Bolte, A., Crowther, T. W., Hansen, M. C., Medlyn, B. E., Ruehr, N. K., & Anderegg,
623 W. R. L. (2018). Monitoring global tree mortality patterns and trends. Report from the
624 VW symposium 'Crossing scales and disciplines to identify global trends of tree
625 mortality as indicators of forest health.' *New Phytologist*, *217*(3), 984–987.
626 https://doi.org/10.1111/nph.14988
627 Hawryło, P., Bednarz, B., Wężyk, P., & Szostak, M. (2018). Estimating defoliation of Scots
628 pine stands using machine learning methods and vegetation indices of Sentinel-2.
629 *European Journal of Remote Sensing*, *51*(1), 194–204.
630 https://doi.org/10.1080/22797254.2017.1417745

631 Hermosilla, T., Bastyr, A., Coops, N. C., White, J. C., & Wulder, M. A. (2022). Mapping the
632 presence and distribution of tree species in Canada's forested ecosystems. *Remote*
633 *Sensing of Environment*, *282*, 113276. https://doi.org/10.1016/j.rse.2022.113276
634 Huang, Z., Turner, B. J., Dury, S. J., Wallis, I. R., & Foley, W. J. (2004). Estimating foliage
635 nitrogen concentration from HYMAP data using continuum removal analysis. *Remote*
636 *Sensing of Environment*, *93*(1–2), 18–29. https://doi.org/10.1016/j.rse.2004.06.008
637 IGN. (2019). *BD Forêt version 2*. Institut National de l'Information Géographique et
638 Forestière. https://inventaire-forestier.ign.fr/spip.php?article646
639 Jackson, R. D., & Huete, A. R. (1991). Interpreting vegetation indices. *Preventive Veterinary*
640 *Medicine*, *11*(3–4), 185–200. https://doi.org/10.1016/S0167-5877(05)80004-2
641 Kamińska, A., Lisiewicz, M., Stereńczak, K., Kraszewski, B., & Sadkowski, R. (2018).
642 Species-related single dead tree detection using multi-temporal ALS data and CIR
643 imagery. *Remote Sensing of Environment*, *219*, 31–43.
644 https://doi.org/10.1016/j.rse.2018.10.005
645 Kautz, M., Peter, F. J., Harms, L., Kammen, S., & Delb, H. (2023). Patterns, drivers and
646 detectability of infestation symptoms following attacks by the European spruce bark
647 beetle. *Journal of Pest Science*, *96*(1), 403–414. https://doi.org/10.1007/s10340-022-
648 01490-8
649 Kennedy, R. E., Yang, Z., & Cohen, W. B. (2010). Detecting trends in forest disturbance and
650 recovery using yearly Landsat time series: 1. LandTrendr — Temporal segmentation
651 algorithms. *Remote Sensing of Environment*, *114*(12), 2897–2910.
652 https://doi.org/10.1016/j.rse.2010.07.008
653 Kokaly, R. F., Asner, G. P., Ollinger, S. V., Martin, M. E., & Wessman, C. A. (2009).
654 Characterizing canopy biochemistry from imaging spectroscopy and its application to

ecosystem studies. *Remote Sensing of Environment*, *113*, S78–S91. https://doi.org/10.1016/j.rse.2008.10.018

König, S., Thonfeld, F., Förster, M., Dubovyk, O., & Heurich, M. (2023). Assessing Combinations of Landsat, Sentinel-2 and Sentinel-1 Time series for Detecting Bark Beetle Infestations. *GIScience & Remote Sensing*, *60*(1), 2226515. https://doi.org/10.1080/15481603.2023.2226515

Lambert, J., Drenou, C., Denux, J.-P., Balent, G., & Cheret, V. (2013). Monitoring forest decline through remote sensing time series analysis. *GIScience & Remote Sensing*, *50*(4), 437–457. https://doi.org/10.1080/15481603.2013.820070

Lastovicka, J., Svec, P., Paluba, D., Kobliuk, N., Svoboda, J., Hladky, R., & Stych, P. (2020). Sentinel-2 Data in an Evaluation of the Impact of the Disturbances on Forest Vegetation. *Remote Sensing*, *12*(12), 1914. https://doi.org/10.3390/rs12121914

Lausch, A., Erasmi, S., King, D., Magdon, P., & Heurich, M. (2017). Understanding Forest Health with Remote Sensing-Part II—A Review of Approaches and Data Models. *Remote Sensing*, *9*(2), 129. https://doi.org/10.3390/rs9020129

Lee, H.-S., & Lee, K.-S. (2019). Multi-temporal Analysis of High-resolution Satellite Images for Detecting and Monitoring Canopy Decline by Pine Pitch Canker. *Korean Journal of Remote Sensing*, *35*(4), 545–560. https://doi.org/10.7780/KJRS.2019.35.4.5

Manion, P. D. (1981). *Tree disease concepts*. Prentice-Hall.

Marx, A., & Kleinschmit, B. (2017). Sensitivity analysis of RapidEye spectral bands and derived vegetation indices for insect defoliation detection in pure Scots pine stands. *IForest - Biogeosciences and Forestry*, *10*(4), 659–668. https://doi.org/10.3832/ifor1727-010

McFeeters, S. K. (1996). The use of the Normalized Difference Water Index (NDWI) in the delineation of open water features. *International Journal of Remote Sensing*, *17*(7), 1425–1432. https://doi.org/10.1080/01431169608948714

Meddens, A. J. H., Hicke, J. A., Vierling, L. A., & Hudak, A. T. (2013). Evaluating methods to detect bark beetle-caused tree mortality using single-date and multi-date Landsat imagery. *Remote Sensing of Environment*, *132*, 49–58. https://doi.org/10.1016/j.rse.2013.01.002

Meiforth, J. J., Buddenbaum, H., Hill, J., & Shepherd, J. (2020). Monitoring of Canopy Stress Symptoms in New Zealand Kauri Trees Analysed with AISA Hyperspectral Data. *Remote Sensing*, *12*(6), 926. https://doi.org/10.3390/rs12060926

Meneghini, A., Rahimzadeh-Bajgiran, P., Livingston, W., & Weiskittel, A. (2022). Detecting White Pine Needle Damage through Satellite Remote Sensing. *Canadian Journal of Remote Sensing*, *48*(2), 239–257. https://doi.org/10.1080/07038992.2021.2023317

Millennium Ecosystem Assessment. (2005). *Ecosystems and human well-being: Synthesis; a report of the Millennium Ecosystem Assessment*. Island Press.

Mouret, F., Morin, D., Martin, H., Planells, M., & Vincent-Barbaroux, C. (2024). Toward an Operational Monitoring of Oak Dieback With Multispectral Satellite Time Series: A Case Study in Centre-Val De Loire Region of France. *IEEE Journal of Selected Topics in Applied Earth Observations and Remote Sensing*, *17*, 643–659. https://doi.org/10.1109/JSTARS.2023.3332420

Pedregosa, F., Varoquaux, G., Gramfort, A., Michel, V., Thirion, B., Grisel, O., Blondel, M., Prettenhofer, P., Weiss, R., Dubourg, V., Vanderplas, J., Passos, A., & Cournapeau, D. (2011). Scikit-learn: Machine Learning in Python. *MACHINE LEARNING IN PYTHON*.

Piedallu, C., Gégout, J., Lebourgeois, F., & Seynave, I. (2016). Soil aeration, water deficit, nitrogen availability, acidity and temperature all contribute to shaping tree species distribution in temperate forests. *Journal of Vegetation Science*, *27*(2), 387–399. https://doi.org/10.1111/jvs.12370

Pontius, J., & Hallett, R. (2014). Comprehensive Methods for Earlier Detection and Monitoring of Forest Decline. *Forest Science*, *60*(6), 1156–1163. https://doi.org/10.5849/forsci.13-121

Radeloff, V. C., Mladenoff, D. J., & Boyce, M. S. (1999). Detecting Jack Pine Budworm Defoliation Using Spectral Mixture Analysis. *Remote Sensing of Environment*, *69*(2), 156–169. https://doi.org/10.1016/S0034-4257(99)00008-5

Rautiainen, M., Lukeš, P., Homolová, L., Hovi, A., Pisek, J., & Mõttus, M. (2018). Spectral Properties of Coniferous Forests: A Review of In Situ and Laboratory Measurements. *Remote Sensing*, *10*(2), 207. https://doi.org/10.3390/rs10020207

Seidl, R., Thom, D., Kautz, M., Martin-Benito, D., Peltoniemi, M., Vacchiano, G., Wild, J., Ascoli, D., Petr, M., Honkaniemi, J., Lexer, M. J., Trotsiuk, V., Mairota, P., Svoboda, M., Fabrika, M., Nagel, T. A., & Reyer, C. P. O. (2017). Forest disturbances under climate change. *Nature Climate Change*, *7*(6), 395–402. https://doi.org/10.1038/nclimate3303

Senf, C., Buras, A., Zang, C. S., Rammig, A., & Seidl, R. (2020). Excess forest mortality is consistently linked to drought across Europe. *Nature Communications*, *11*(1), 6200. https://doi.org/10.1038/s41467-020-19924-1

Senf, C., Pflugmacher, D., Zhiqiang, Y., Sebald, J., Knorn, J., Neumann, M., Hostert, P., & Seidl, R. (2018). Canopy mortality has doubled in Europe's temperate forests over the last three decades. *Nature Communications*, *9*(1), 4978. https://doi.org/10.1038/s41467-018-07539-6

Strona, G., Mauri, A., & San-Miguel-Ayanz, J. (2016). *A high-resolution pan-European tree occurrence dataset*. Figshare. https://doi.org/10.6084/M9.FIGSHARE.C.3288407.V1

Taccoen, A., Piedallu, C., Seynave, I., Perez, V., Gégout-Petit, A., Nageleisen, L.-M., Bontemps, J.-D., & Gégout, J.-C. (2019). Background mortality drivers of European tree species: Climate change matters. *Proceedings of the Royal Society B: Biological Sciences*, *286*(1900), 20190386. https://doi.org/10.1098/rspb.2019.0386

Torres, P., Rodes-Blanco, M., Viana-Soto, A., Nieto, H., & García, M. (2021). The Role of Remote Sensing for the Assessment and Monitoring of Forest Health: A Systematic Evidence Synthesis. *Forests*, *12*(8), 1134. https://doi.org/10.3390/f12081134

Trumbore, S., Brando, P., & Hartmann, H. (2015). Forest health and global change. *Science*, *349*(6250), 814–818. https://doi.org/10.1126/science.aac6759

Tucker, C. J. (1979). Red and photographic infrared linear combinations for monitoring vegetation. *Remote Sensing of Environment*, *8*(2), 127–150. https://doi.org/10.1016/0034-4257(79)90013-0

UNECE & FAO (Ed.). (2011). *Forest Europe*. Ministerial Conference on the Protection of Forests in Europe.

Verbesselt, J., Hyndman, R., Newnham, G., & Culvenor, D. (2010). Detecting trend and seasonal changes in satellite image time series. *Remote Sensing of Environment*, *114*(1), 106–115. https://doi.org/10.1016/j.rse.2009.08.014

Vidal, C., Be, T., & Wolsack, J. (2005). *A New Flexible Forest Inventory in France*.

Vogelmann, J. E., & Rock, B. N. (1988). Assessing forest damage in high-elevation coniferous forests in vermont and new Hampshire using thematic mapper data. *Remote Sensing of Environment*, *24*(2), 227–246. https://doi.org/10.1016/0034-4257(88)90027-2

751 White, J., Wulder, M., Brooks, D., Reich, R., & Wheate, R. (2005). Detection of red attack
752 stage mountain pine beetle infestation with high spatial resolution satellite imagery.
753 *Remote Sensing of Environment*, *96*(3–4), 340–351.
754 https://doi.org/10.1016/j.rse.2005.03.007
755 Woodcock, C. E., Loveland, T. R., Herold, M., & Bauer, M. E. (2020). Transitioning from
756 change detection to monitoring with remote sensing: A paradigm shift. *Remote*
757 *Sensing of Environment*, *238*, 111558. https://doi.org/10.1016/j.rse.2019.111558
758 Ye, S., Rogan, J., Zhu, Z., Hawbaker, T. J., Hart, S. J., Andrus, R. A., Meddens, A. J. H.,
759 Hicke, J. A., Eastman, J. R., & Kulakowski, D. (2021). Detecting subtle change from
760 dense Landsat time series: Case studies of mountain pine beetle and spruce beetle
761 disturbance. *Remote Sensing of Environment*, *263*, 112560.
762 https://doi.org/10.1016/j.rse.2021.112560
763

764